Research Article

Media development and process parameter optimization using statistical experimental designs for the production of nonribosomal peptides in *Escherichia coli*

Arne Michael Oestreich [a], Merlinda Ilire Suli [a], Doreen Gerlach [a,c], Rong Fan [a,c,*], Peter Czermak [a,b,c,*]

[a] *Institute of Bioprocess Engineering and Pharmaceutical Technology, University of Applied Sciences Mittelhessen, 35390 Giessen, Germany*
[b] *Faculty of Biology and Chemistry, Justus-Liebig University of Giessen, 35390 Giessen, Germany*
[c] *Fraunhofer Institute for Molecular Biology and Applied Ecology, Project Group Bioresources, 35390 Giessen, Germany*

ARTICLE INFO

ABSTRACT

Background: Nonribosomal peptide synthases (NRPS) can synthesize functionally diverse bioactive peptides by incorporating nonproteinogenic amino acids, offering a rich source of new drug leads. The bacterium *Escherichia coli* is a well-characterized production host and a promising candidate for the synthesis of nonribosomal peptides, but only limited bioprocess engineering has been reported for such molecules. We therefore developed a medium and optimized process parameters using the design of experiments (DoE) approach.
Results: We found that glycerol is not suitable as a carbon source for rhabdopeptide production, at least for the NRPS used for this study. Alternative carbon sources from the tricarboxylic acid cycle achieved much higher yields. DoE was used to optimize the pH and temperature in a stirred-tank reactor, revealing that optimal growth and optimal production required substantially different conditions.
Conclusions: We developed a chemically defined adapted M9 medium matching the performance of complex medium (lysogeny broth) in terms of product concentration. The maximum yield in the reactor under optimized conditions was 126 mg L^{-1}, representing a 31-fold increase compared to the first shaking-flask experiments with M9 medium and glycerol as the carbon source. Conditions that promoted cell growth tended to inhibit NRPS productivity. The challenge was therefore to find a compromise between these factors as the basis for further process development.
How to cite: Oestreich AM, Suli LI, Gerlach D. et al. Media development and process parameter optimization using statistical experimental designs for the production of nonribosomal peptides in *Escherichia coli*. Electron J Biotechnol 2021;52. https://doi.org/10.1016/j.ejbt.2021.05.001

1. Introduction

Multidrug-resistant microbes pose an increasing threat to healthcare systems due to the indiscriminate use of antibiotics, creating a demand for new antimicrobial drugs with novel mechanisms of action [1]. One promising approach is the use of nonribosomal peptides, which are microbial secondary metabolites produced by modular enzyme complexes known as nonribosomal peptide synthases (NRPS) [2,3]. Many nonribosomal peptides are bioactive, with pharmacological properties that include antibiotic, immunosuppressive and cytotoxic activities [4,5,6,7,8,9,10,11]. The ability of NRPS to utilize a variety of substrates, including nonpro-

teinogenic amino acids [6,12], produces a range of nonribosomal peptides with remarkable structural diversity, representing an evolutionary advantage in a rapidly changing environment. For example, a symbiotic relationship has evolved between bacteria (*Xenorhabdus* spp.) and entomopathogenic nematodes of the family *Steinernematidae* in which the bacteria supply the nematodes with rhabdopeptides/xenortides (RXP) that support the reproductive success [13]. RXPs are linear peptides, usually 2–8 amino acids in length with a C–terminal amine [13]. The NRPS used in this study (VietABC) originates from *Xenorhabdus vietnamensis* and produces a nonribosomal peptide consisting of three *N*-methylated leucine residues and a terminal amine [13].

The efficient production of nonribosomal peptides in cultivated bacteria requires a growth medium that not only promotes cell growth but also favors the activity of NRPS. Ideally, the medium

---

should also be chemically defined in order to meet the requirements of good manufacturing practice (GMP), reduce the cost of raw materials (by replacing components such as peptones with inexpensive salts) and simplify downstream processing. Several well-established chemically defined media have been optimized for the growth of *Escherichia coli* (*E. coli*), but not for nonribosomal peptide production. Process parameters such as temperature and pH have been shown to influence the productivity of NRPS [14,15,16,17], but the optimal conditions for VietABC synthase have not been established. It is therefore necessary to optimize the production process for temperature, pH and substrate concentration in the medium in order to balance cell growth and productivity.

The testing of growth conditions one factor at a time is inefficient because it does not account for interactions between factors. In contrast, the Design of Experiments (DoE) approach is a systematic method to determine the significant factors and interactions that influence the behavior of a system, allowing multiple factors to be optimized simultaneously. The aim of such statistical experimental designs is the precise representation of the relationship between the influence factors (independent variables) that are investigated and the response factors (dependent variables) with high significance and low experimental effort. Modeling is based on a regression whose function is valid in the entire design space. The DoE not only models and predicts the effects of independent variables but also predicts the necessary resources, such as substrates, time and other cost factors [18]. Response surface methodology (RSM) is a DoE approach that describes models on the basis of polynomial functions, identifying nonlinear relationships between dependent and independent variables. The goal of RSM is to find existing extrema (maxima and minima) as well as saddle points, and to identify optimal settings for the process [19]. The application of RSM requires knowledge of statistically significant independent variables, which are best determined by screening different conditions in factorial designs [18]. Different RSM design types can be used for optimization depending on the structure of the model, including central composite, Box–Behnken and optimal designs.

2. Materials and methods

2.1. Production strain and vectors

The leucine auxotroph strain *E. coli* DH10B was kindly provided by Prof. Dr. Helge B. Bode (Institute for Molecular Biosciences, Goethe University Frankfurt, Germany). This strain contains two plasmids (pCX71 and pACYC) in which genes are regulated by the arabinose (*ara*) operon: pCX71 (18,055 bp) carries the VietABC biosynthetic gene cluster and a kanamycin-resistance gene, whereas pACYC (4689 bp) carries phosphopantetheinyl transferase (*mtaA*) and chloramphenicol acetyltransferase genes.

2.2. Culture medium

We developed a modified M9 mineral medium [20] containing 33.7 mM Na_2HPO_4, 22 mM KH_2PO_4, 8.55 mM NaCl, 9.35 mM NH_4Cl, 54.3 mM glycerol, 0.75 mM L-leucine, 1 mM $MgSO_4$, 0.3 mM $CaCl_2$, 342 μM EDTA, 31 μM $FeCl_3$, 6.2 μM $ZnCl_2$, 0.76 μM $CuCl_2$, 0.42 μM $CoCl_2$, 1.62 μM H_3BO_3 and 0.081 μM $MnCl_2$. A stock solution containing all trace elements except $FeCl_3$ (due to poor stability) was prepared with half the amount of EDTA. The rest was used for the $FeCl_3$ stock. NRPS expression was induced with 25 mM arabinose. For product formation, we added 1 mM phenethylamine (PEA). We also added kanamycin sulfate (60 μM) and chloramphenicol (105.2 μM) to maintain selection pressure. Each tricar-

boxylic acid (TCA) cycle intermediate of the carbon source screening was provided as a dibasic sodium salt, set to an equimolar carbon content of 5 g L^{-1} glycerol. All chemicals were obtained from Sigma-Aldrich (Taufkirchen, Germany), Merck (Darmstadt, Germany) or Carl Roth (Karlsruhe, Germany). Stocks and media were prepared using ultra-pure water with a resistivity of 18.2 MΩ cm at 25 °C. Stock solutions were autoclaved for 20 min at 121 °C or filter-sterilized using 0.22 μm polyether sulfone filters.

2.3. Shaking flask cultivation

Cells were cultivated in 300-mL flasks containing 30 mL of culture medium at 30 °C, shaking at 125 rpm (5 cm orbit). Cryopreserved cultures were used to inoculate the medium to an initial ΔOD_{600} of 0.2. The cultures were incubated for at least 24 h or until the cells reached stationary phase.

2.4. Reactor cultivation

MiniBio 500 stirred-tank reactors (Applikon Biotechnology, Delft, Netherlands) with a working volume of 300 mL, equipped with a micro sparger and pH, temperature and dissolved oxygen sensors, were part filled with a solution of Na_2HPO_4, KH_2PO_4, NaCl and NH_4Cl and autoclaved for 20 min at 121 °C. The remaining components of the adapted M9 medium were then added via syringe. Fermentations were carried out with an initial ΔOD_{600} of 0.2 at an aeration rate of 1 vvm and a stirrer speed of 1000 rpm. Experiments were stopped when the cells reached stationary phase. The pH was controlled by adding 2 M HCl.

2.5. Measurement of cell density

Cell density was measured with a BioSpectrometer basic (Eppendorf, Hamburg, Germany) at a wavelength of 600 nm. The signal was linear in the ΔOD_{600} range 0.05–0.3. To fit this range, samples with higher ΔOD_{600} were diluted with 0.9% NaCl. Cell dry weight (CDW) was calculated based on an experimentally determined correlation between ΔOD_{600} and CDW.

2.6. RXP quantification

The product concentration was measured by ultrahigh-performance liquid chromatography (UHPLC) on a Dionex Ultimate 3000 and Corona Veo RS detector (Thermo Fisher Scientific, Dreieich, Germany) fitted with an Acquity UPLC BEH C18 column (130 Å, 1.7 μm, 2.1 mm × 100 mm) (Waters, Eschborn, Germany). RXP prepared by solid-phase synthesis and verified by mass spectrometry, kindly provided by Prof. Dr. Helge B. Bode (Institute for Molecular Biosciences, Goethe University Frankfurt, Germany) was used as the calibration standard. Ultrapure water and acetonitrile supplemented with 0.1% (v/v) formic acid were used as solvents. Analysis was carried at 40 °C with a flow rate of 0.4 mL min^{-1}. The initial acetonitrile concentration of 5% was held for 3 min before a three-step linear increase (5–30% in 0.8 min, 30–55% in 7.2 min, and 55–95% in 1 min). The acetonitrile concentration was then held at 95% for 4 min before reducing it to 5% in 1 min and re-equilibrating for 3 min. To protect the Corona Veo RS detector from ions, the flow state was switched off for the first 3 min of each measurement. Fermentation broth samples were centrifuged for 20 min at 16,100 × g and transferred to glass vials for analysis.

2.7. SDS-PAGE

Chemical cell lysis of 1 to 1.5 mL cell suspension was conducted using BugBuster master mix (Merck Millipore, Darmstadt, Germany). Samples of 15 μL were mixed with 4.5 μL Laemmli buffer

and 0.5 μL 2-mercaptoethanol and heated for 5 min to 95 °C. Subsequently 12 μL of the treated samples were transferred to 4–20% Criterion TGX stain free precast gels (Bio-Rad Laboratories, Hercules, USA). Gels were run for 26 min at 250 volt in electrophorese chambers filled with TGS buffer. Precision Plus Unstained Protein Standard (Bio-Rad Laboratories, Hercules, USA) was run in first (2 μL) and last (4 μL) lane. Analysis of protein gels were done with ChemiDoc MP imaging system and Image Lab software (Bio-Rad Laboratories, Hercules, USA).

2.8. Design of experiments

Experimental designs were generated and evaluated using Design Expert v11 (Stat-Ease, Minneapolis, MN, USA). Media development was based on a randomized RSM, I-optimal quadratic design (n = 27) in shaking flasks. We considered concentration ranges of 0.3–30 mM for NH_4Cl, 0.05–2.5 mM for L-leucine, and 4–200 mM for succinate. The influence of pH (5.75–8.25) and temperature (20–35 °C) was investigated using a randomized RSM, I-optimal, quadratic design (n = 21) in three parallel stirred-tank reactors, and was thus divided into three blocks.

The quality of all models met the requirements for sufficient navigation in the design space and the models were used for point prediction. Each model was evaluated in confirmation runs. Models were generated with significant influence factors and interactions. To maintain hierarchical model arrangement, non-significant influence factors or interactions of a lower order were implemented as long as a corresponding significant interaction of a higher order was added to the design.

Experimental designs, analysis of variance and coefficients in terms of coded factors can be found in the supplementary information supplementary data

3. Results and discussion

3.1. Carbon source screening

Experiments carried out using lysogeny broth (LB) as a complex medium achieved an RXP concentration of 59.1 ± 3.2 mg L^{-1} whereas M9 medium containing glycerol as the carbon source was much less productive (4.0 ± 0.2 mg L^{-1}). This suggested the presence of beneficial components in the LB medium or inhibitory components in the M9 medium. To clarify this issue, we cultivated the bacteria in terrific broth (TB) supplemented with 5 g L^{-1} glycerol. It was found that product formation was inhibited as long as glycerol was present in the fermentation medium even though intense bands of the NRPS were detectable on a SDS-PAGE (data not shown). Following the consumption of glycerol, the cells start to utilize amino acids as a carbon and energy source, converting them into tricarboxylic acid (TCA) cycle intermediates. We therefore assumed that the utilization of TCA cycle intermediates does not inhibit RXP production in the same manner as glycerol. Given that NRPS expression is regulated by p$_{BAD}$, carbohydrates cannot be used as a carbon source because they repress the promoter [21].

Fig. 1 shows that some amino acids were totally depleted during the fermentation while others were only consumed in small amounts. Amino acid utilization for energy metabolism increases the concentration of ammonia due to oxidative deamination [22]. Accordingly, ~50% of the amino acids were used as a carbon source and for energy metabolism.

Table 1 shows the TCA cycle intermediates formed when specific amino acids are metabolized. The dibasic salts of these intermediates were used as carbon sources with the same carbon content as 5 g L^{-1} glycerol in shaking-flask experiments. Oxaloacetate was not tested due to high costs, and we used sodium acetate and dis-
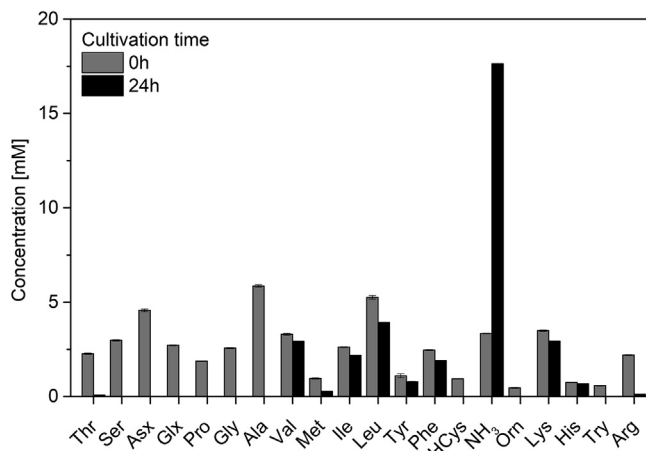

Fig. 1. Initial concentration (0 h) and final concentration (24 h) of amino acids during the cultivation of *E. coli* DH10B in a bioreactor containing TB medium. Asx = asparagine and aspartate; Glx = glutamine and glutamate (n = 3).

Table 1
Amino acids and their conversion into TCA cycle intermediates.

Amino acids	TCA cycle intermediates
Alanine / glycine / serine	Pyruvate
Arginine / glutamine / glutamate / proline	α-Ketoglutarate
Asparagine	Oxaloacetate
Aspartate	Fumarate / oxaloacetate
Methionine	Succinyl-CoA
Threonine / tryptophan	Pyruvate / succinyl-CoA / acetyl-CoA

odium succinate in place of acetyl-CoA and succinyl-CoA, respectively. Acetate and pyruvate as sole carbon sources were insufficient for cell growth, with no growth observed even after 7 d (data not shown).

Cultures supplemented with disodium succinate produced RXP concentrations of up to 25 mg L^{-1}, which is several times higher than the other carbon sources (Fig. 2). Although experiments with fumarate and α-ketoglutarate resulted in low growth rates and low cell densities, the RXP concentration was still higher than that achieved with glycerol. Although glycerol promoted the highest growth rate and maximum ΔOD_{600}, the product concentration was the lowest among the carbon sources we tested. This supports our hypothesis that TCA cycle intermediates do not inhibit product
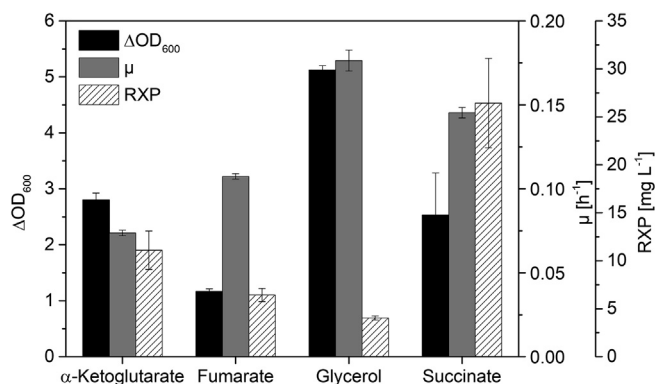

Fig. 2. Carbon source screening for RXP production in *E. coli* DH10B using chemically defined M9 medium in shaking flasks at 30 °C (n = 3).

formation to the extent demonstrated by glycerol, especially in terms of RXP yield per unit biomass.

3.2. Experimental design for the development of M9 medium

We designed a screening for critical media components (NH$_4$Cl, FeCl$_3$, MgSO$_4$ and L-leucine) to determine the factors with a significant influence on product formation and cell growth (data not shown). The effect of succinate was investigated in one factor at a time (OFAT) experiments and was therefore not included in the screening. We found that NH$_4$Cl and L-leucine had a significant influence on growth rate and CDW but NH$_4$Cl had no significant impact on RXP formation (at least within the limits of the model). Design space limits of the M9 DoE model were determined by OFAT experiments.

As shown in Fig. 3, the effect of L-leucine on cell growth was generally negative. The cells have a high substrate affinity, allowing them to grow rapidly even at low substrate concentrations. High concentrations of L-leucine are therefore toxic, and the maximum concentration compatible with the growth of *E. coli* was previously found to be 22.9 mM [23]. However, the inhibitory effect was ameliorated in complex media containing other amino acids [24]. Similarly, in our reactor experiment with complex medium we observed a growth rate of 0.5 h^{-1} when the concentration of L–leucine was about twice as high as the maximum concentration investigated in the M9 DoE. For NH$_4$Cl and succinate, higher concentrations are required to achieve the highest growth rate, suggesting a higher affinity constant.

Although high concentrations of L-leucine had a negative effect on the growth rate, they had a positive effect on the maximum CDW (Fig. 4). This reflects the growth limitation caused by auxotrophy. As soon as L-leucine (used for growth and product formation) is depleted, protein biosynthesis and cell growth stagnates. But if the concentration of L-leucine is too high, cell growth slows and substrates are utilized due to maintenance metabolism and therefore become limited before reaching the maximum cell density or before the culture conditions (such as the pH) become inhibiting. The influence of the remaining substrates follows a similar pattern.

In contrast to the initial screening, NH$_4$Cl had a significant influence on RXP formation because the concentration limits used in

the DoE differed from those in the screening. The local optima of product formation (Fig. 5) were approximately congruent with those of the maximum CDW (Fig. 4). Although previous experiments had shown that inhibiting substrate concentrations have a positive effect on the yield, this involves a biomass-associated weighting. It is unclear whether the data in Fig. 5 agree with the productivity optimum or whether bias is caused by the biomass.

Fig. 6 confirms that inhibiting substrate concentrations have a positive effect on the yield, with the optimum of the RXP concentration (Fig. 5) almost coinciding with the maximum yield (Fig. 6). Increasing the concentration of NH$_4$Cl triggers relative variations in the RXP and biomass concentrations, leading to the mutual equalization of these terms. This is shown by the fact that NH$_4$Cl does not have a significant influence on the RXP yield per unit biomass. A semi quantitative SDS-PAGE showed a linear correlation between VietABC synthase concentration and CDW over the entire design space with R^2 of 0.87, indicating that Fig. 6 displays the activity of the synthase. The optima shown in Fig. 5 are therefore assumed to be suitable initial concentrations for the chemically defined medium. To validate the model, we carried out confirmation runs with 20.2 mM NH$_4$Cl, 1.7 mM L-leucine and 138.6 mM succinate. All response factors determined within the framework of the confirmation runs were consistent with the simulation, and the corresponding models were therefore deemed sufficient for point prediction. An RXP concentration of 55.9 ± 3.93 mg L^{-1} was achieved by media optimization, representing a 14-fold increase over the first experiments with a chemically defined medium. The pH of the medium increased to 9.5 in shaking flasks with succinate as the carbon source. Here, the growth-limiting factor is the pH, which means that a higher CDW (and potentially a higher product concentration) can be anticipated in regulated systems. The product concentrations achieved in reactor cultivations with LB medium were no higher than those observed in the shaking-flask experiments.

3.3. Experimental design to optimize the temperature and pH

We used the optimized M9 medium described above in the subsequent process parameter optimization experiments. The design limits were established based on the results of OFAT experiments. Although the optimum growth temperature for *E. coli* is ~ 37 °C, we
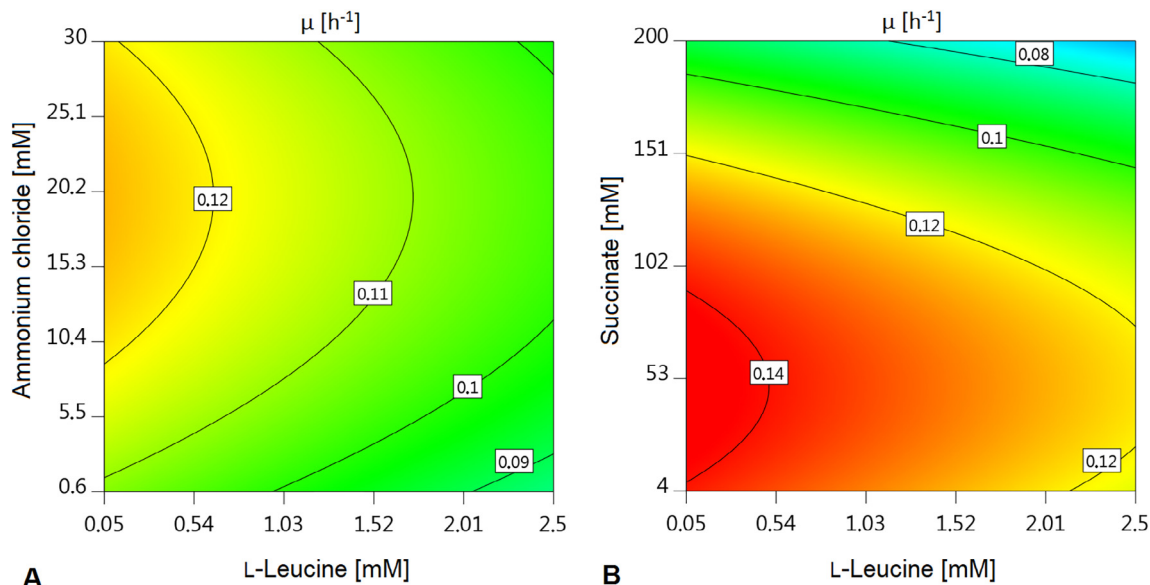

Fig. 3. Contour plots of the growth rate model with the influence factors (A) NH$_4$Cl and L-leucine, or (B) succinate and L-leucine (model p-value < 0.0001, lack of fit p-value = 0.2583, R^2 = 0.96, adjusted R^2 = 0.95, predicted R^2 = 0.92, adequate precision = 35.22).
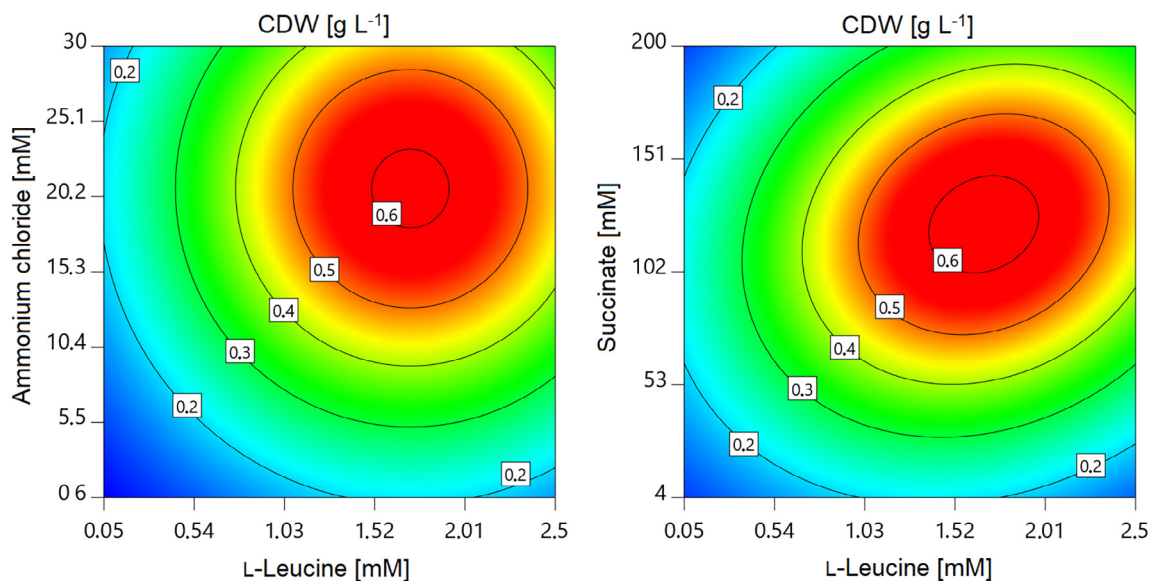
Fig. 4. Contour plots of the CDW model with the influence factors (A) NH$_4$Cl and L-leucine, or (B) succinate and L-leucine (model p-value < 0.0001, lack of fit p-value = 0.0003, R^2 = 0.92, adjusted R^2 = 0.89, predicted R^2 = 0.79, adequate precision = 16.44).
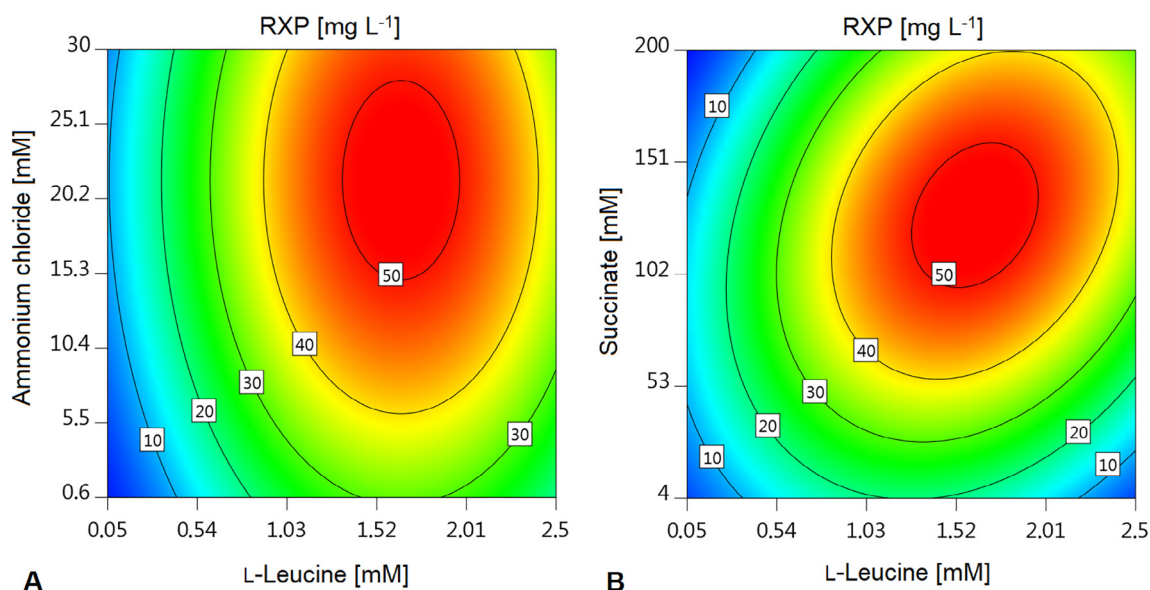
Fig. 5. Contour plots of the RXP concentration model with the influence factors (A) NH$_4$Cl and L-leucine, or (B) succinate and L-leucine (model p-value < 0.0001, lack of fit p-value = 0.0641, R^2 = 0.86, adjusted R^2 = 0.81, predicted R^2 = 0.71, adequate precision = 13.10).

chose an upper limit of 35 °C to avoid losing degrees of freedom in the RXP design because no product formation was detected at higher temperatures.

Maximum cell densities were predicted within the temperature range 32–35 °C and the pH range 6–7. The model suggested that the optimum was beyond the temperature range, reflecting the mesophilic nature of *E. coli* with its optimum growth temperature of ~ 37 °C [25,26]. The pH also influenced the maximum cell density, reflecting the need for *E. coli* to maintain an intracellular pH of 7.2–7.8 (homeostasis) regardless of the extracellular pH, in order to ensure that its proteins and nucleic acids remain stable [27]. The intracellular pH is regulated by various ion transporters, which enable bacteria to grow in environments with more extreme pH ranges [28]. The model confirmed that *E. coli* DH10B cells tolerate environmental pH values within the investigated limits (pH 5.75–

8.25) and suggested that the tolerance of alkaline pH decreases with increasing temperature (Fig. 7). The opposite effect was observed for slightly acidic pH values, which indicates a complex interaction between these parameters.

The contour plot in Fig. 8 shows maximum growth rates (μ ≈ 0.17 h^{-1}) within the temperature range 32–35 °C and the pH range 6.5–7.5. Low temperatures such as 20 °C result in minimal growth rates (<0.05 h^{-1}) with little dependence on pH.

The reduced cubic model in Fig. 9 suggests that pH values below 7 achieve a higher product concentration. Maximum product concentrations of > 120 mg L^{-1} can be expected at ~ 27 °C within the pH range 6.0–6.8, suggesting that enzyme activity increases under these conditions. High temperatures may cause incorrect folding of the VietABC synthase domains leading to inclusion body formation, thus resulting in a low concentration of RXP, but no further infor-
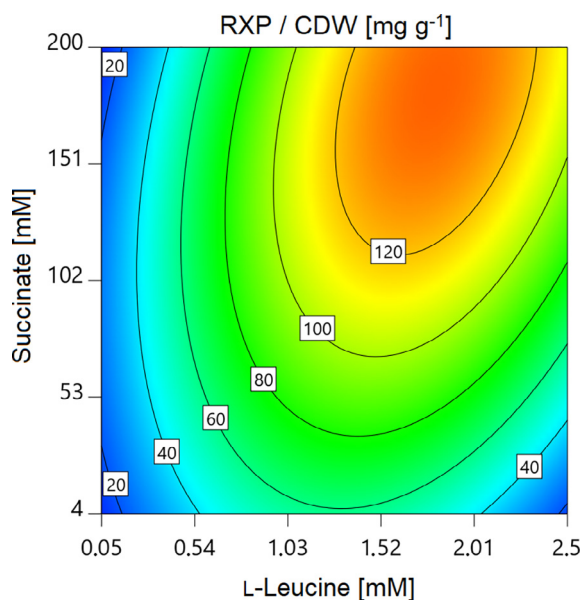
Fig. 6. Contour plot of the RXP yield per CDW model with the influence factors succinate and L-leucine (model p-value < 0.0001, lack of fit p-value = 0.5465, R^2 = 0.86, adjusted R^2 = 0.82, predicted R^2 = 0.77, adequate precision = 13.79).
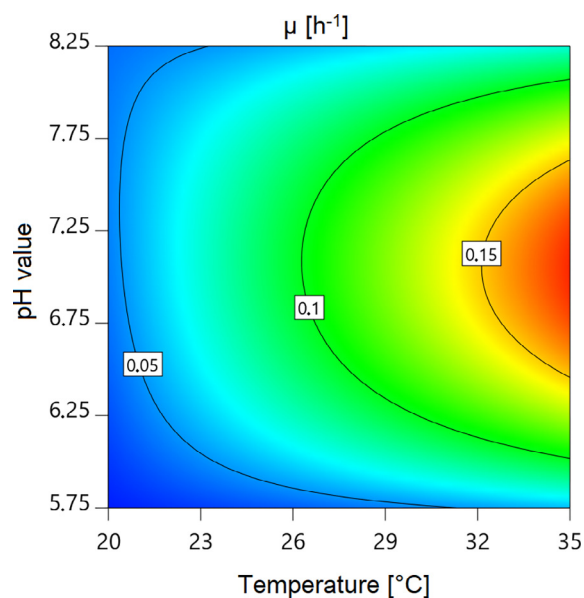

Fig. 8. Contour plot of the growth rate model with the influence factors pH and temperature (model p-value < 0.0001, lack of fit p-value = 0.0822, R^2 = 0.93, adjusted R^2 = 0.90, predicted R^2 = 0.84, adequate precision = 17.54).
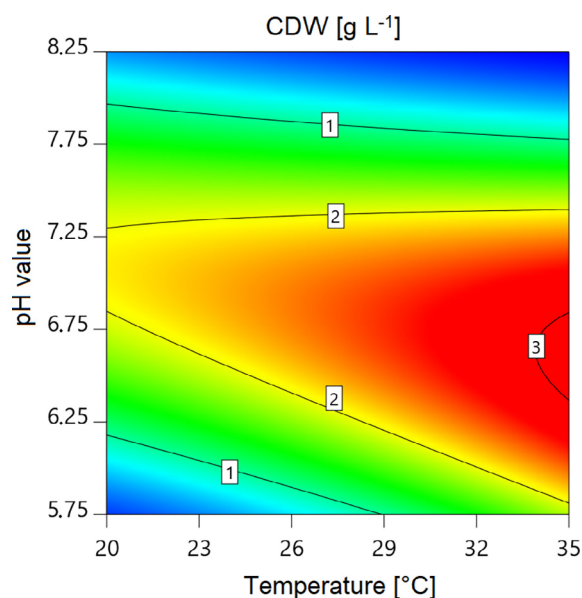

Fig. 7. Contour plot of the CDW model with the influence factors pH and temperature (model p-value < 0.0001, lack of fit p-value = 0.0300, R^2 = 0.94, adjusted R^2 = 0.92, predicted R^2 = 0.84, adequate precision = 17.41).
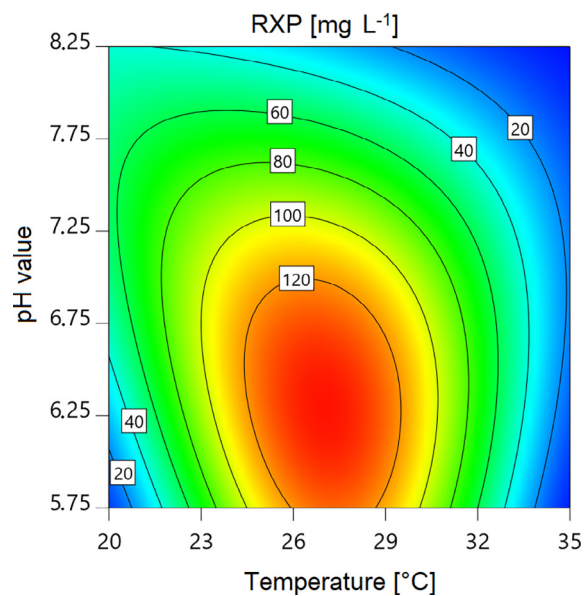

Fig. 9. Contour plot of the RXP concentration model with the influence factors pH and temperature (model p-value < 0.0001, lack of fit p-value = 0.3233, R^2 = 0.93, adjusted R^2 = 0.89, predicted R^2 = 0.72, adequate precision = 12.55).

mation is available concerning the optimum pH and temperature of this enzyme. Furthermore, because arabinose uptake involves the proton-coupled symporter AraE [21], a slightly acidic medium may promote the uptake of inducer molecules and thus increase the expression of the biosynthetic gene cluster, resulting in higher product concentrations.

Maximum productivity occurred at 29 °C and neutral pH, a compromise between biomass accumulation and enzyme activity (Fig. 10). The optimal conditions for product formation therefore differ significantly from those required for optimal growth. Confirmation runs carried out at 27 °C and pH 6.4 achieved an RXP concentration of 126.07 ± 14.28 mg L^{-1} and a maximum productivity of 3.21 mg L^{-1} h^{-1} with a CDW of 1.81 ± 0.13 g L^{-1} at a growth rate of

0.099 ± 0.003 h^{-1} (n = 3). In comparison, confirmation runs at 29 °C and pH 7.0 achieved an RXP concentration of 117.37 ± 6.63 mg L^{-1} and a maximum productivity of 4.43 mg L^{-1} h^{-1} with a CDW of 2.14 ± 0.04 g L^{-1} at a growth rate of 0.116 ± 0.012 h^{-1} (n = 3). Although the first set of conditions achieved a slightly higher product concentration, the second set of conditions achieved a higher productivity and the process time was reduced by 25%. All simulated variables agreed with the results of the confirmation runs and the models were therefore deemed sufficient for point prediction.

Table 2 shows the relatively low concentration of heterologous nonribosomal peptides produced by fermentation in *E. coli* growing in chemically defined media. However, these values are only com-
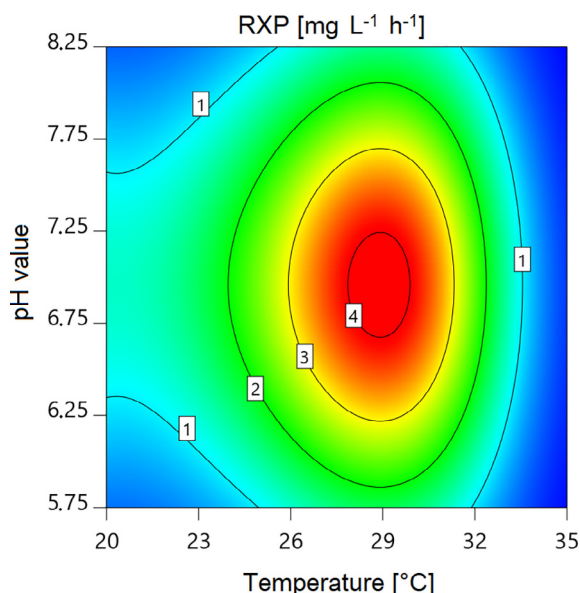
RXP [mg L⁻¹ h⁻¹]

Fig. 10. Contour plot of the RXP productivity model with the influence factors pH and temperature (model p-value < 0.0001, lack of fit p-value = 0.1459, R^2 = 0.91, adjusted R^2 = 0.87, predicted R^2 = 0.77, adequate precision = 12.85).

Table 2
Heterologous production of nonribosomal peptides by *E. coli* in chemically defined media using different process modes.

Process mode	Product	c_p [mg L⁻¹]
Fed-batch reactor cultivation	Echinomycin	0.3 [29]
Batch cultivation in shaking-flasks	Ecolimycin C	0.6 [30]
Sequential fed-batch in shaking-flasks	Triostin A	13 [31]

parable to our results in a limited sense, because they are based on different products and process modes. We achieved product titers ~ 10-fold higher than these previous studies, but more optimization would be required for an industrial-scale process where product titers in the two digit gram range are needed for economic viability [32].

4. Conclusions

Although chemically defined media tend to deliver lower nonribosomal peptide titers than complex media [14,29,30,31,33,34, 35,36], with some exceptions, a chemically defined medium was developed that can compete with LB medium in terms of RXP production in shaking-flask fermentations. Reactor cultivations with LB medium did not increase the RXP concentration compared to shaking-flaks experiments any further, but the chemically defined medium doubled the product titer (to 126 mg L⁻¹) in a regulated system. This equates to a 31–fold increase in product concentration compared to the non-optimized medium and process parameters in shaking flasks (4.0 ± 0.2 mg L⁻¹). The optimal conditions of 29 °C and pH 7 reflected the higher growth rate, shorter process time and higher productivity, and offer a promising starting point for the development of a fed-batch process. The process described herein outperformed the other reported *E. coli* fermentation process for nonribosomal peptides using chemically defined medium by ~ 10–fold [31]. Due to the slow growth under optimal production conditions and the associated long process time, a two-phase fed–batch process with a shift in process parameters may be the most suitable approach in terms of economic viability and product titers.

Supplementary material

https://doi.org/10.1016/j.ejbt.2021.05.001.

References

[1] Meyer E, Gastmeier P, Deja M, et al. Antibiotic consumption and resistance: data from Europe and Germany. Int J Med Microbiol 2013;303(6–7):388–95. https://doi.org/10.1016/j.ijmm.2013.04.004 PMid: 23727396.
[2] Finking R, Marahiel MA. Biosynthesis of nonribosomal peptides1. Annu Rev Microbiol 2004;58:453–88. https://doi.org/10.1146/annurev. micro.58.030603.123615 PMid: 15487945.
[3] Walsh CT. The chemical versatility of natural-product assembly lines. Acc Chem Res 2008;41(1):4–10. https://doi.org/10.1021/ar7000414 PMid: 17506516.
[4] Balibar CJ, Vaillancourt FH, Walsh CT. Generation of D amino acid residues in assembly of arthrofactin by dual condensation/epimerization domains. Chem Biol 2005;12(11):1189–200. https://doi.org/10.1016/j.chembiol.2005.08.010 PMid: 16298298.
[5] Baltz RH, Miao V, Wrigley SK. Natural products to drugs: daptomycin and related lipopeptide antibiotics. Nat Prod Rep 2005;22(6):717–41. https://doi. org/10.1039/b416648p PMid: 16311632.
[6] Caboche S, Leclère V, Pupin M, et al. Diversity of monomers in nonribosomal peptides: towards the prediction of origin and biological activity. J Bacteriol 2010;192(19):5143–50. https://doi.org/10.1128/JB.00315-10 PMid: 20693331.
[7] Calcott MJ, Ackerley DF. Genetic manipulation of non-ribosomal peptide synthetases to generate novel bioactive peptide products. Biotechnol Lett 2014;36(12):2407–16. https://doi.org/10.1007/s10529-014-1642-y PMid: 25214216.
[8] Du L, Lou L. PKS and NRPS release mechanisms. Nat Prod Rep 2010;27 (2):255–78. https://doi.org/10.1039/B912037H PMid: 20111804.
[9] Felnagle EA, Jackson EE, Chan YA, et al. Nonribosomal peptide synthetases involved in the production of medically relevant natural products. Mol Pharm 2008;5(2):191–211. https://doi.org/10.1021/mp700137g PMid: 18217713.
[10] Lawen A. Biosynthesis of cyclosporins and other natural peptidyl prolyl cis/trans isomerase inhibitors. BBA 2015;1850(10):2111–20. https://doi.org/ 10.1016/j.bbagen.2014.12.009 PMid: 25497210.
[11] Sieber SA, Marahiel MA. Molecular mechanisms underlying nonribosomal peptide synthesis: approaches to new antibiotics. Chem Rev 2005;105 (2):715–38. https://doi.org/10.1021/cr0301191 PMid: 15700962.
[12] Grünewald J, Marahiel MA. Chemoenzymatic and template-directed synthesis of bioactive macrocyclic peptides. Microbiol Mol Biol Rev 2006;70(1):121–46. https://doi.org/10.1128/MMBR.70.1.121-146.2006 PMid: 16524919.
[13] Cai X, Nowak S, Wesche F, et al. Entomopathogenic bacteria use multiple mechanisms for bioactive peptide library design. Nat Chem 2017;9(4):379–86. https://doi.org/10.1038/nchem.2671 PMid: 28338679.
[14] Gruenewald S, Mootz HD, Stehmeier P, et al. *In vivo* production of artificial nonribosomal peptide products in the heterologous host *Escherichia coli*. Appl Environ Microbiol 2004;70(6):3282–91. https://doi.org/10.1128/ AEM.70.6.3282-3291.2004 PMid: 15184122.
[15] Kranzler M, Stollewerk K, Rouzeau-Szynalski K, et al. Temperature Exerts Control of Bacillus cereus Emetic Toxin Production on Post-transcriptional Levels. Front Microbiol 2016;7:1640. https://doi.org/10.3389/ fmicb.2016.01640 PMid: 27826288.
[16] Yuan B, Liu D, Guan X, et al. Piperazine ring formation by a single-module NRPS and cleavage by an α-KG-dependent nonheme iron dioxygenase in brasiliamide biosynthesis. Appl Microbiol Biotechnol 2020;104(14):6149–59. https://doi.org/10.1007/s00253-020-10678-w PMid: 32436033.

[17] Zeng J, Zhan J. Characterization of a tryptophan 6-halogenase from *Streptomyces toxytricini*. Biotechnol Lett 2011;33(8):1607–13. https://doi.org/10.1007/s10529-011-0595-7 PMid: 21424165.

[18] Montgomery DC. Design and analysis of experiments. 8. ed. Hoboken, NJ: Wiley; 2013.

[19] Bezerra MA, Santelli RE, Oliveira EP, et al. Response surface methodology (RSM) as a tool for optimization in analytical chemistry. Talanta 2008;76(5):965–77. https://doi.org/10.1016/j.talanta.2008.05.019 PMid: 18761143.

[20] Geerlof A. M9 mineral medium. Helmholtz Center Munich 2010. Available from Internet: https://www.helmholtz-muenchen.de/fileadmin/PEPF/Protocols/M9-medium_150510.pdf

[21] Schleif R. Regulation of the l-arabinose operon of *Escherichia coli*. Trends Genet 2000;16(12):559–65. https://doi.org/10.1016/S0168-9525(00)02153-3.

[22] Hossain GS, Li J, Shin HD, et al. L-Amino acid oxidases from microbial sources: types, properties, functions, and applications. Appl Microbiol Biotechnol 2014;98(4):1507–15. https://doi.org/10.1007/s00253-013-5444-2 PMid: 24352734.

[23] Beckmann B, Hohmann D, Eickmeyer M, et al. An improved high cell density cultivation-iHCDC-strategy for leucine auxotrophic *Escherichia coli* K12 ER2507. Eng Life Sci 2017;17(8):857–64. https://doi.org/10.1002/elsc.201700054 PMid: 32624833.

[24] Rowley D. Inhibition of E. coli strains by amino-acids. Nature 1953;171(4341):80–81. https://doi.org/10.1038/171080a0 PMid: 13025488

[25] Doyle MP, Schoeni JL. Survival and growth characteristics of *Escherichia coli* associated with hemorrhagic colitis. Appl Environ Microbiol 1984;48(4):855–6. https://doi.org/10.1128/AEM.48.4.855-856.1984 PMid: 6391379.

[26] O'Donovan GA, Kearney CL, Ingraham JL. Mutants of *Escherichia coli* with High Minimal Temperatures of Growth. J Bacteriol 1965;90(3):611–6. https://doi.org/10.1128/JB.90.3.611-616.1965 PMid: 16562056.

[27] Wilks JC, Slonczewski JL. pH of the cytoplasm and periplasm of *Escherichia coli*: rapid measurement by green fluorescent protein fluorimetry. J Bacteriol 2007;189(15):5601–7. https://doi.org/10.1128/JB.00615-07 PMid: 17545292.

[28] Booth IR. Regulation of cytoplasmic pH in bacteria. Microbiol Rev 1985;49(4):359–78. https://doi.org/10.1128/MR.49.4.359-378.1985.

[29] Watanabe K, Hotta K, Praseuth AP, et al. Total biosynthesis of antitumor nonribosomal peptides in *Escherichia coli*. Nat Chem Biol 2006;2(8):423–8. https://doi.org/10.1038/nchembio803 PMid: 16799553.

[30] Watanabe K, Hotta K, Nakaya M, et al. *Escherichia coli* allows efficient modular incorporation of newly isolated quinomycin biosynthetic enzyme into echinomycin biosynthetic pathway for rational design and synthesis of potent antibiotic unnatural natural product. J Am Chem Soc 2009;131(26):9347–53. https://doi.org/10.1021/ja902261a PMid:19514719.

[31] Praseuth AP, Praseuth MB, Oguri H, et al. Improved production of triostin A in engineered *Escherichia coli* with furnished quinoxaline chromophore by design of experiments in small-scale culture. Biotechnol Prog 2008;24(1):134–9. https://doi.org/10.1021/bp070298y PMid: 18173279.

[32] Li J, Neubauer P. *Escherichia coli* as a cell factory for heterologous production of nonribosomal peptides and polyketides. New Biotechnol 2014;31(6):579–85. https://doi.org/10.1016/j.nbt.2014.03.006 PMid: 24704144.

[33] Bozhüyük KAJ, Linck A, Tietze A, et al. Modification and de novo design of non-ribosomal peptide synthetases using specific assembly points within condensation domains. Nat Chem 2019;11(7):653–61. https://doi.org/10.1038/s41557-019-0276-z PMid: 31182822.

[34] Li J, Jaitzig J, Hillig F, et al. Enhanced production of the nonribosomal peptide antibiotic valinomycin in Escherichia coli through small-scale high cell density fed-batch cultivation. Appl Microbiol Biotechnol 2014;98(2):591–601. https://doi.org/10.1007/s00253-013-5309-8 PMid: 24419900.

[35] Ongley SE, Bian X, Zhang Y, et al. High-titer heterologous production in E. coli of lyngbyatoxin, a protein kinase C activator from an uncultured marine cyanobacterium. ACS chemical biology 2013;8(9):1888–1893. https://doi.org/10.1021/cb400189j PMid: 23751865

[36] Wyatt MA, Magarvey NA. Optimizing dimodular nonribosomal peptide synthetases and natural dipeptides in an *Escherichia coli* heterologous host. Biochem Cell Biol 2013;91(4):203–8. https://doi.org/10.1139/bcb-2012-0097 PMid: 23859013.